Numerical simulations of the electromagnetic field scattered by defects in a double-periodic structure

Patrick C. Chaumet and Anne Sentenac
Institut Fresnel (UMR 6133), Université Paul Cézanne, Avenue Escadrille Normandie-Niemen, F-13397 Marseille cedex 20, France
(Received 21 June 2005; revised manuscript received 29 September 2005; published 23 November 2005)

We have developed a rigorous numerical method that permits the simulation of the electromagnetic field scattered by an aperiodic object in presence of a double-periodic structure (grating). Our volume integral formulation, which is an extension of the classic coupled dipole method, is versatile and can address inhomogeneous objects and gratings of any shape. The electromagnetic field is calculated both in the near-field and far-field region. In this latter case we propose an efficient technique based on the reciprocity theorem.

DOI: 10.1103/PhysRevB.72.205437 PACS number(s): 42.25.Fx, 41.20.−q, 02.70.Dh

I. INTRODUCTION

Development of numerical tools that simulate the electromagnetic field inside complex structures is crucial for the understanding of physical phenomena and the design of new components. The study of the interaction between the electromagnetic field and an object placed in the vicinity of a planar periodic structure has many applications. For example, it permits one to evaluate the field enhancement inside microcavities in photonic crystal slabs, to calculate the scattering by grating defects, or to simulate the radiation pattern of sources in a structured planar waveguide.[1]

Several numerical techniques have been proposed to solve the Maxwell equations without any approximation except that necessary for the numerical implementation. Among these are the finite difference time domain method (FDTD), the finite element method (FEM), the multiple multipole method (MMP), the volume integral equation [such as the coupled dipole method (CDM) or method of moment (MoM)], the surface integral equation.[2] However, despite the progress of the computing capabilities, these techniques are usually adapted to specific configurations to limit the calculation cost. Hence the evaluation of the field scattered by a bounded three-dimensional object immersed in an homogeneous space will not be addressed in the same way as that of the field scattered by an infinite periodic structure (or grating).[3]

In our configuration, the structure is an aperiodic object (defect) in the presence of a double-periodic structure (grating), hence it is neither periodic nor bounded and few simulation tools are adapted to this problem. If one assumes that the defect is duplicated periodically (with a period much larger than that of the grating), codes adapted to periodic structures, such as the differential or coupled-wave methods,[4] can be used. This supercell technique gives an accurate result if the defect period is large enough so that the coupling between adjacent objects can be neglected. In general this leads to a large number of unknowns in the Fourier field representation and a very high computation cost. FDTD techniques with periodic boundary conditions can also be proposed.[5] In this case, the discretized domain must be large enough so that the influence of the defect at the edges is negligible.[6,7]

In this paper we propose an efficient method that simulates the field scattered by a defect in a two-dimensional periodic structure without invoking the supercell technique. Our approach is an extension of the coupled dipole method or equivalently the method of moment.[8] One first calculates the field susceptibility tensor of the grating which gives the field scattered by a dipole in the presence of the double-periodic structure. In this work, the tensor is obtained through a volume integral formulation which can address inhomogeneous gratings of any shapes. Then, the aperiodic object is considered as a collection of dipoles whose exciting field is obtained by solving a self-consistent linear system involving the field susceptibility tensor of the grating. Last, when the local field inside the aperiodic object is known, the scattered field is evaluated in the near-field and far-field regions. Since the CDM is a volume integral equation method, it can address any arbitrary shaped, inhomogeneous, anisotropic defect and periodic structure. Another important advantage of this technique is that its numerical cost lies essentially in the calculation of the field susceptibility tensor. Once the latter is evaluated and memorized, one can easily study the scattering by various objects (for example, different kinds of microcavities). The additional numerical effort will be the same as that obtained if the objects were in a homogeneous medium.

Our paper is organized as follows: In Sec. II A the principles of the coupled dipole method are developed. The calculation of the field susceptibility tensor of the double-periodic structure is given in Sec. II B, and the field scattered in far field is investigated in Sec. II C. In Sec. II D we show how this method can be used to calculate the scattering by a lacuna of the grating. Section III is devoted to some numerical results and comparisons with other techniques, and we draw our conclusion in Sec. IV.

II. COMPUTATION OF THE DIFFRACTED FIELD BY A DEFECT IN A PERIODIC STRUCTURE

A. Formalism of the problem

In its original form, the coupled dipole method (CDM) was developed to study the free-space scattering of light by an object with finite dimensions.[9,10] The method was subse-

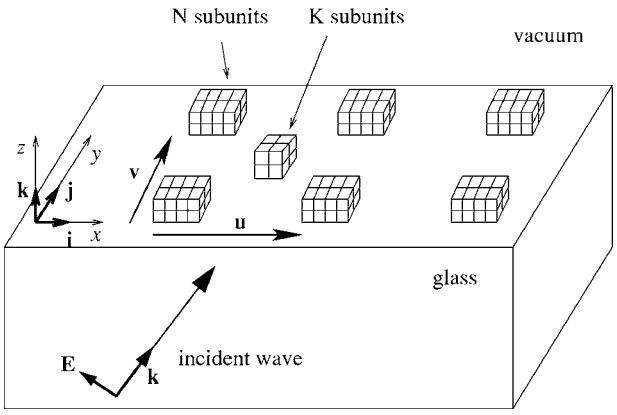

FIG. 1. Geometry of the system: double-periodic structure with basis vector **u** and **v**. The base cell of the periodic structure is discretized in *N* subunits. In this periodic structure a defect is introduced, and is discretized in *K* subunits. The double-periodic structure and the defect are above a flat substrate.

quently extended to deal with objects near a substrate[11,12] or inside a multilayer system.[13] Recently the CDM has been extended to planar periodic structures or gratings.[3] Now we consider the scattering by an aperiodic object deposited on a grating (Fig. 1). More precisely, in our configuration, a planar homogeneous substrate occupies the region $z \leqslant 0$ and the grating and object occupy the region $z > 0$. The grating is made of a motif (or base cell) that is duplicated periodically on the substrate. The whole structure is illuminated by a plane wave which comes either from the substrate or the superstrate. In the coupled dipole method, the objects are represented by a cubic array of polarizable subunits, each with a size small enough compared to the spatial variations of the electromagnetic field for the dipole approximation to apply. Hence, in our configuration, the local electric field at the *i*th subunit at location $\mathbf{r}_i$ is given by the self-consistent equation,

$$\begin{aligned}\mathbf{E}(\mathbf{r}_i) = \mathbf{E}^0(\mathbf{r}_i) &+ \sum_{j=1}^{N} \sum_{m,n=-\infty}^{\infty} [\mathbf{H}(\mathbf{r}_i, \bar{\mathbf{r}}_j + m\mathbf{u} + n\mathbf{v}) \\ &+ \mathbf{F}(\mathbf{r}_i, \bar{\mathbf{r}}_j + m\mathbf{u} + n\mathbf{v})]\alpha_{\mathrm{p}}(\bar{\mathbf{r}}_j)\mathbf{E}(\bar{\mathbf{r}}_j + m\mathbf{u} + n\mathbf{v}) \\ &+ \sum_{k=1}^{K} [\mathbf{H}(\mathbf{r}_i, \mathbf{r}_k) + \mathbf{F}(\mathbf{r}_i, \mathbf{r}_k)]\alpha_{\mathrm{d}}(\mathbf{r}_k)\mathbf{E}(\mathbf{r}_k), \end{aligned} \tag{1}$$

where $\Sigma_{m,n=-\infty}^{\infty}$ means that we perform a double sum, i.e., $\Sigma_{m=-\infty}^{\infty}\Sigma_{n=-\infty}^{\infty}$. The index *i* runs over all the subunits of the structure (grating and defect). **F** is the free-space field susceptibility[14] and **H** represents the field susceptibility associated with the surface.[13] The aperiodic object (or defect) is discretized into *K* subunits located at $\mathbf{r}_k$ with $k = 1, \ldots, K$ and polarizability $\alpha_{\mathrm{d}}(\mathbf{r}_k)$. The elementary motif of the grating (restricted to one period) is discretized into *N* subunits placed at $\bar{\mathbf{r}}_j$ with $j = 1, \ldots, N$ and polarizability $\alpha_{\mathrm{p}}(\bar{\mathbf{r}}_j)$. The whole grating is described by an infinite set of dipoles, placed at $\bar{\mathbf{r}}_j + m\mathbf{u} + n\mathbf{v}$ with $(m,n) \in \mathbb{Z}^2$. $(\mathbf{u}, \mathbf{v})$ is the period of the grating with $\mathbf{u} = u_x\mathbf{i} + u_y\mathbf{j}$ and $\mathbf{v} = v_x\mathbf{i} + v_y\mathbf{j}$. The expression of the polarizability of each subunit is given by

$$\alpha_{\mathrm{d,p}}(\mathbf{r}_i) = \alpha^0_{\mathrm{d,p}}(\mathbf{r}_i)/[1 - (2/3)ik_0^3\alpha^0_{\mathrm{d,p}}(\mathbf{r}_i)], \tag{2}$$

where the lower index d, p denotes the polarizability associated with the defect or the period respectively. k_0 is the modulus of the wave vector of the electromagnetic field in vacuum, and $\alpha^0_{\mathrm{d,p}}(\mathbf{r}_i)$ satisfies the Clausius-Mossotti relation :

$$\alpha^0_{\mathrm{d,p}}(\mathbf{r}_i) = \frac{3d^3_{\mathrm{d,p}}}{4\pi} \frac{\varepsilon_{\mathrm{d,p}}(\mathbf{r}_i) - 1}{\varepsilon_{\mathrm{d,p}}(\mathbf{r}_i) + 2}. \tag{3}$$

In Eq. (3) $d_{\mathrm{d,p}}$ is the spacing of the object discretization (defect or grating) and $\varepsilon_{\mathrm{d,p}}(\mathbf{r}_i)$ stands for its relative permittivity. The term $(2/3)ik_0^3\alpha^0_{\mathrm{d,p}}(\mathbf{r}_i)$ in Eq. (2) is related to the radiative reaction term and is essential to satisfy the optical theorem.[15,16] Note that the the contact term $\mathbf{F}(\mathbf{r}_i, \mathbf{r}_i)$ in Eq. (1) is equal to zero inasmuch as we are dealing with the local electric field.[8] In Eq. (1), due to the grating, the number of subunits is infinite, and therefore so is the size of the linear system to be solved. One solution would be to truncate the infinite sum, and solve the system for a large but finite number of objects, but this is impractical because the sums over the lattice converge very slowly.

This problem can be circumvented by taking the substrate and the grating as the reference system of the problem. To this aim, one introduces the field susceptibility tensor of the double periodic structure **G**, such that $\mathbf{G}(\mathbf{r}, \mathbf{r}')\mathbf{p}(\mathbf{r}')$ is the electric field at $\mathbf{r}$ radiated by a dipole $\mathbf{p}(\mathbf{r}')$ placed at $\mathbf{r}'$ in presence of the grating. With this tool, one can calculate the local field inside the aperiodic object through a self-consistent integral equation. Namely, the local field is the sum of the field that would exist in absence of the defect $\mathbf{E}_{\mathrm{per}}(\mathbf{r})$ (this field can be obtained with any classic grating method; in Appendix A and B we provide a means to calculate it with the CDM formalism), plus the field radiated *in the presence of the grating* by the *K* dipoles forming the aperiodic object. The self-consistent equation giving the local field inside the aperiodic object reads

$$\mathbf{E}(\mathbf{r}_i) = \mathbf{E}_{\mathrm{per}}(\mathbf{r}_i) + \sum_{k=1}^{K} \mathbf{G}(\mathbf{r}_i, \mathbf{r}_k)\alpha_{\mathrm{d}}(\mathbf{r}_k)\mathbf{E}(\mathbf{r}_k). \tag{4}$$

Equation (4) is a linear system to solve whose size is $3K \times 3K$. Once the local field $\mathbf{E}(\mathbf{r}_i)$ is known at each $\mathbf{r}_i$, for $i = 1, \ldots, K$ the electric field can be computed everywhere outside the aperiodic object through the equation

$$\mathbf{E}(\mathbf{r}) = \mathbf{E}_{\mathrm{per}}(\mathbf{r}) + \sum_{k=1}^{K} \mathbf{G}(\mathbf{r}, \mathbf{r}_k)\alpha_{\mathrm{d}}(\mathbf{r}_k)\mathbf{E}(\mathbf{r}_k). \tag{5}$$

From Eqs. (4) and (5), it appears that the main difficulty of the CDM is to calculate the field susceptibility tensor of the periodic structure.

B. Field susceptibility tensor of a double-periodic structure

Very few techniques have been proposed to calculate the field susceptibility tensor of a periodic structure. In Ref. 1 one calculates the field scattered by a dipole placed in a grating with an *S*-matrix approach and the use of the Fourier modal method. This method is efficient when the field inside

the periodic structure can be represented adequately by a small number of Fourier coefficients, i.e., when the period of the grating is small. In this paper, we use a volume integral approach which is efficient when the grating motif can be described by a small number of dipoles, regardless of the period. The field susceptibility tensor $\mathbf{G}(\mathbf{r},\mathbf{r}')$ which gives the field in $\mathbf{r}$ radiated by a dipole placed in $\mathbf{r}'$ in presence of the grating is written as the sum of the field radiated by the dipole in presence of the substrate alone with the field radiated by the infinite number of subunits periodically placed on the substrate and constituting the grating:

$$\mathbf{G}(\mathbf{r},\mathbf{r}') = \mathbf{S}(\mathbf{r},\mathbf{r}') + \sum_{j=1}^{N}\sum_{m,n=-\infty}^{\infty} \mathbf{S}(\mathbf{r},\bar{\mathbf{r}}_j + m\mathbf{u} + n\mathbf{v}) \times \alpha_p(\bar{\mathbf{r}}_j)\mathbf{G}(\bar{\mathbf{r}}_j + m\mathbf{u} + n\mathbf{v},\mathbf{r}'), \quad (6)$$

with $\mathbf{S}(\mathbf{r},\mathbf{r}')=\mathbf{F}(\mathbf{r},\mathbf{r}')+\mathbf{H}(\mathbf{r},\mathbf{r}')$ and $(\mathbf{u},\mathbf{v})$ are the basis vectors of the grating. It is worth noting here that one could replace the field susceptibility tensor of the surface by the field susceptibility tensor of a multilayer. It amounts to changing the Fresnel reflection and transmission coefficients present in the expression of $\mathbf{H}$ by that of the multilayer. In the same way, we can remove the substrate with $\mathbf{H}=0$.

To compute $\mathbf{G}(\mathbf{r},\mathbf{r}')$ we define a new tensor as

$$\mathbf{G}_{per}(\mathbf{r},\mathbf{r}',\mathbf{k}_\parallel) := \sum_{p,q=-\infty}^{\infty} \mathbf{G}(\mathbf{r}+p\mathbf{u}+q\mathbf{v},\mathbf{r}') \times \exp[i\mathbf{k}_\parallel . (p\mathbf{u}+q\mathbf{v})], \quad (7)$$

where the tensor $\mathbf{G}_{per}$ is pseudoperiodic with $\mathbf{G}_{per}(\mathbf{r}+m\mathbf{u}+n\mathbf{v},\mathbf{r}',\mathbf{k}_\parallel)=\mathbf{G}_{per}(\mathbf{r},\mathbf{r}',\mathbf{k}_\parallel)\exp[-i\mathbf{k}_\parallel.(m\mathbf{u}+n\mathbf{v})]$. Similarly, we introduce a pseudoperiodic tensor associated with the surface:

$$\mathbf{S}_{per}(\mathbf{r},\mathbf{r}',\mathbf{k}_\parallel) := \sum_{p,q=-\infty}^{\infty} \mathbf{S}(\mathbf{r}+p\mathbf{u}+q\mathbf{v},\mathbf{r}') \times \exp[i\mathbf{k}_\parallel . (p\mathbf{u}+q\mathbf{v})]. \quad (8)$$

Notice that this new tensor $\mathbf{S}_{per}$, as detailed in Refs. 3,17, can be computed very efficiently. Due to the translational invariance of the substrate $\mathbf{S}_{per}$ has some properties, notably we have $\mathbf{S}_{per}(\mathbf{r}+p\mathbf{u}+q\mathbf{v},\mathbf{r}',\mathbf{k}_\parallel)=\mathbf{S}_{per}(\mathbf{r},-p\mathbf{u}-q\mathbf{v}+\mathbf{r}',\mathbf{k}_\parallel)=\mathbf{S}_{per}(\mathbf{r},\mathbf{r}',\mathbf{k}_\parallel)\exp[-i\mathbf{k}_\parallel.(p\mathbf{u}+q\mathbf{v})]$.

Introducing Eq. (6) in Eq. (7) and using the definition of Eq. (8) and the property of $\mathbf{S}_{per}$, Eq. (7) can be written as

$$\mathbf{G}_{per}(\mathbf{r},\mathbf{r}',\mathbf{k}_\parallel) = \mathbf{S}_{per}(\mathbf{r},\mathbf{r}',\mathbf{k}_\parallel) + \sum_{j=1}^{N} \mathbf{S}_{per}(\mathbf{r},\bar{\mathbf{r}}_j,\mathbf{k}_\parallel) \times \alpha_p(\bar{\mathbf{r}}_j)\mathbf{G}_{per}(\bar{\mathbf{r}}_j,\mathbf{r}',\mathbf{k}_\parallel). \quad (9)$$

To obtain $\mathbf{G}_{per}(\mathbf{r},\mathbf{r}',\mathbf{k}_\parallel)$ from Eq. (9), one needs to compute $\mathbf{G}_{per}(\bar{\mathbf{r}}_j,\mathbf{r}',\mathbf{k}_\parallel)$ which is the solution of the following self-consistent equation:

$$\mathbf{G}_{per}(\bar{\mathbf{r}}_k,\mathbf{r}',\mathbf{k}_\parallel) = \mathbf{S}_{per}(\bar{\mathbf{r}}_k,\mathbf{r}',\mathbf{k}_\parallel) + \sum_{j=1}^{N} \mathbf{S}_{per}(\bar{\mathbf{r}}_k,\bar{\mathbf{r}}_j,\mathbf{k}_\parallel) \times \alpha_p(\bar{\mathbf{r}}_j)\mathbf{G}_{per}(\bar{\mathbf{r}}_j,\mathbf{r}',\mathbf{k}_\parallel). \quad (10)$$

Equation (10) is a linear system of equation of size $3N \times 3N$ where $\mathbf{G}_{per}(\bar{\mathbf{r}}_k,\mathbf{r}',\mathbf{k}_\parallel)$ are the unknowns. Once this system is solved, $\mathbf{G}_{per}(\mathbf{r},\mathbf{r}',\mathbf{k}_\parallel)$ can be obtained for any position $\mathbf{r}$ and $\mathbf{r}'$.

Now, the pseudoperiodic $\mathbf{G}_{per}(\mathbf{r},\mathbf{r}',\mathbf{k}_\parallel)$ [Eq. (7)] can be cast into a Fourier series whose elements are given by the following integral:

$$\mathbf{G}(\mathbf{r},\mathbf{r}'+m\mathbf{u}+n\mathbf{v}) = \frac{1}{S}\int\int_S \mathbf{G}_{per}(\mathbf{r},\mathbf{r}',\mathbf{k}_\parallel) \times \exp[-i\mathbf{k}_\parallel . (m\mathbf{u}+n\mathbf{v})]d\mathbf{k}_\parallel \quad (11)$$

where $\int\int_S$ means that the integration is performed over the first Brillouin zone of the grating, defined by the two following vectors:

$$\mathbf{U} = 2\pi(v_y\mathbf{i} - v_x\mathbf{j})/(u_xv_y - v_xu_y), \quad (12)$$

$$\mathbf{V} = 2\pi(-u_y\mathbf{i} + u_x\mathbf{j})/(u_xv_y - v_xu_y), \quad (13)$$

and $S=|\mathbf{U}\times\mathbf{V}|$. Hence taking $(m,n)=(0,0)$ Eq. (11) leads to the following expression for the field tensor susceptibility of the double periodic structure:

$$\mathbf{G}(\mathbf{r},\mathbf{r}') = \frac{1}{S}\int\int_S \mathbf{G}_{per}(\mathbf{r},\mathbf{r}',\mathbf{k}_\parallel)d\mathbf{k}_\parallel. \quad (14)$$

The tensor $\mathbf{G}$ is then obtained through Eq. (14) which is discretized for numerical purposes as

$$\mathbf{G}(\mathbf{r},\mathbf{r}') \approx \frac{1}{MM'}\sum_{l=0}^{M-1}\sum_{l'=0}^{M'-1} \mathbf{G}_{per}\left(\mathbf{r},\mathbf{r}',\frac{l}{M}\mathbf{U}+\frac{l'}{M'}\mathbf{V}\right), \quad (15)$$

with (M,M') a natural positive number. Note that this discretization has a physical meaning. Indeed, the field susceptibility tensor obtained with Eq. (15) is doubly periodical with periods equal to $M\mathbf{u}$ and $M'\mathbf{v}$. In the other term, it gives the field in $\mathbf{r}$ radiated by an infinite set of dipoles placed at $\mathbf{r}'+lM\mathbf{u}+l'M'\mathbf{v}$ where $(l,l')\in\mathbb{Z}^2$. The larger (M,M') the better the approximation for the tensor. Hence we are faced with the same problem of convergence as that encountered in a supercell method.[6] At this point, it is worth stressing that the field radiated by a dipole in the presence of a grating is the sum of the field radiated by the dipole in the presence of the bare substrate (given by $\mathbf{S}$) plus the field radiated by each subunits forming the grating. To minimize the influence of the field radiated by the discretization-induced dipoles we calculate the field susceptibility tensor by injecting Eq. (9) in Eq. (14), while using Eq. (8). We obtain

$$\mathbf{G}(\mathbf{r},\mathbf{r}') = \mathbf{S}(\mathbf{r},\mathbf{r}') + \frac{1}{S}\int\int_S \sum_{j=1}^{N} [\mathbf{S}_{per}(\mathbf{r},\bar{\mathbf{r}}_j,\mathbf{k}_\parallel) \times \alpha_p(\bar{\mathbf{r}}_j)\mathbf{G}_{per}(\bar{\mathbf{r}}_j,\mathbf{r}',\mathbf{k}_\parallel)]d\mathbf{k}_\parallel, \quad (16)$$

$$\approx \mathbf{S}(\mathbf{r},\mathbf{r}') + \frac{1}{MM'}\sum_{l=0}^{M-1}\sum_{l'=0}^{M'-1}\sum_{j=1}^{N}\left[\mathbf{S}_{\mathrm{per}}\left(\mathbf{r},\overline{\mathbf{r}}_j,\frac{l}{M}\mathbf{U}+\frac{l'}{M'}\mathbf{V}\right)\right.$$
$$\left.\times\,\alpha_{\mathrm{p}}(\overline{\mathbf{r}}_j)\mathbf{G}_{\mathrm{per}}\left(\overline{\mathbf{r}}_j,\mathbf{r}',\frac{l}{M}\mathbf{U}+\frac{l'}{M'}\mathbf{V}\right)\right], \quad (17)$$

where $\mathbf{G}_{\mathrm{per}}(\overline{\mathbf{r}}_j,\mathbf{r}',\mathbf{k}_{\parallel})$ is obtained from Eq. (10). With this formulation, the calculation of $\mathbf{S}$ is independent of the discretization due to the numerical procedure. Hence, at the observation point, the field radiated by the dipole via the bare substrate is accurately accounted for. The unwanted contribution of the discretization-induced dipoles located at $\mathbf{r}'+lM\mathbf{u}+l'M'\mathbf{v}$ is solely felt through multiple scattering with the subunits of the grating. It is worth noting that the field radiated in $\mathbf{r}$ by the discretization-induced dipoles will be significantly smaller than that radiated by the "real" dipole placed at $\mathbf{r}'$ if $|\mathbf{r}-\mathbf{r}'|\ll\min(|\mathbf{r}-\mathbf{r}'-M\mathbf{u}|,|\mathbf{r}-\mathbf{r}'-M'\mathbf{v}|)$.

C. Evaluation of the field in the far-field zone

The method presented in Sec. II B to calculate the field susceptibility tensor is not efficient if the position of observation $\mathbf{r}$ is located in the far-field zone. Indeed, to minimize the contribution of the discretization-induced dipoles, Eq. (17), one should have $|\mathbf{r}|\ll\min(|M\mathbf{u}|,|M'\mathbf{v}|)$, which is impossible when $|\mathbf{r}|$ is very large compared to the wavelength. In this case, it is much simpler and efficient to use the reciprocity theorem to calculate the tensor. The latter states that, whatever the configuration under study (and, in particular, in presence of the grating) the field $\mathbf{E}'(\mathbf{r}_k)$ created by a dipole $\mathbf{p}'$ placed at $\mathbf{r}$ is related to the field $\mathbf{E}(\mathbf{r})$ created by a dipole $\mathbf{p}$ placed at $\mathbf{r}_k$ through the relation[18]

$$\mathbf{p}(\mathbf{r}_k)\cdot\mathbf{E}'(\mathbf{r}_k)=\mathbf{p}'(\mathbf{r})\cdot\mathbf{E}_k(\mathbf{r}). \quad (18)$$

Now, the field scattered by the dipole $\mathbf{p}'$ placed at $\mathbf{r}$ in far field and impinging on the defect embedded in the grating can be written as

$$\mathbf{E}^0(\mathbf{r}_k)=\mathbf{p}'_{\perp}(\mathbf{r})\frac{e^{ik_0|\mathbf{r}-\mathbf{r}_k|}}{|\mathbf{r}-\mathbf{r}_k|}\approx\mathbf{p}'_{\perp}(\mathbf{r})\frac{e^{ik_0|\mathbf{r}|}}{|\mathbf{r}|}e^{-i\mathbf{k}_0\cdot\mathbf{r}_k}, \quad (19)$$

where $\mathbf{p}'_{\perp}(\mathbf{r})$ means that we take only the component of the dipole moment perpendicular to the vector $\mathbf{r}$ and $\mathbf{k}_0=k_0\mathbf{r}/r$. Hence $\mathbf{E}^0$ can be assimilated to an incident plane wave with magnitude $e^{ik_0|\mathbf{r}|}/|\mathbf{r}|$. To compute the field $\mathbf{E}'(\mathbf{r}_k)$ we use Eqs. (5) and (A1) where the incident field $\mathbf{E}^0$ is replaced by the expression given by Eq. (19). Once $\mathbf{E}'(\mathbf{r}_k)$ is evaluated for the two fundamental polarizations it is easy to compute $\mathbf{E}_k(\mathbf{r})$ from Eq. (18). Finally, to obtain the field diffracted by the object in the presence of the grating in far field, we add the field contribution of each dipole forming the object as

$$\mathbf{E}(\mathbf{r})=\mathbf{E}_{\mathrm{per}}(\mathbf{r})+\sum_{k=1}^{K}\mathbf{E}_k(\mathbf{r}). \quad (20)$$

D. Particular case where the defect is a lacuna in the double-periodic structure

The method that we have presented can be used to create a lacuna in the double-periodic structure. In this case, the aperiodic object must have exactly the same discretization as that of the grating motif and the same polarizability with opposite sign: $\alpha_{\mathrm{d}}(\overline{\mathbf{r}}'_j)=-\alpha_{\mathrm{p}}(\overline{\mathbf{r}}_j+m\mathbf{u}+m'\mathbf{v})$ for $j=1,\ldots,N$ [it is obvious from Eq. (1) that the resulting structure will be a grating with a missing motif]. For example, the field scattered by a grating whose central motif has been suppressed, i.e., $(m,n)=(0,0)$ which implies $\overline{\mathbf{r}}'_j=\overline{\mathbf{r}}_j$, is given by

$$\mathbf{E}(\mathbf{r})=\mathbf{E}_{\mathrm{per}}(\mathbf{r})+\sum_{k=1}^{N}\mathbf{G}(\mathbf{r},\overline{\mathbf{r}}_k)\alpha_{\mathrm{d}}(\overline{\mathbf{r}}_k)\mathbf{E}(\overline{\mathbf{r}}_k), \quad (21)$$

$$\mathbf{E}(\overline{\mathbf{r}}_k)=\mathbf{E}_{\mathrm{per}}(\overline{\mathbf{r}}_k)+\sum_{l=1}^{N}\mathbf{G}(\overline{\mathbf{r}}_k,\overline{\mathbf{r}}_l)\alpha_{\mathrm{d}}(\overline{\mathbf{r}}_l)\mathbf{E}(\overline{\mathbf{r}}_l), \quad (22)$$

where $\mathbf{E}_{\mathrm{per}}(\overline{\mathbf{r}}_k)$ is obtained with Eq. (A1) and the field susceptibility tensor of the grating $\mathbf{G}$ is given by Eq. (17). In Eq. (21) the sum over k represents the field scattered by the defect with the negative polarizability, i.e., the difference between the field scattered by the periodic structure minus the field scattered by the structure with the lacuna. Obviously, with the same technique, it is also possible to displace or to change the nature of one base cell of the grating.

III. NUMERICAL RESULTS

In this section, we present some numerical results and we check the convergence of our method. We consider a double-periodic structure made of silicon cubes of width a deposited along a square lattice of period $\mathbf{u}=(p,0)$ and $\mathbf{v}=(0,p)$ on a glass substrate. The aperiodic object is a cube of silver with the same width a, placed at the center of the square cell [see Figs. 2(a) and 2(b)]. The substrate is illuminated from the substrate, with a TM polarized plane wave with angle of incidence θ [see Figs. 2(b)], and the magnitude of the incident field is set to 1. The angle of incidence can be chosen so as to illuminate the grating in total internal reflection. In the first example, we have taken $a=50$ nm, $p=200$ nm, and $\lambda=600$ nm. The relative permittivity of the material are taken from Palik's handbook.[19] Figures 2(c) and 2(d) show the modulus of the electromagnetic field calculated at an altitude $h=100$ nm for an angle of incidence $\theta=0°$ and $\theta=50°$, respectively. These figures show clearly the coupling between the silver defect and the neighboring silicon cubes and the limits of its influence. Within a few periods away from the defect, the field is not affected by its presence. In this example, the calculation has been done for $M=M'=11$, and one can wonder if the convergence is obtained. In the next example we study the influence of the number of modes (M,M') on the accuracy of the results. In Figs. 3(a) and 3(b), we plot the near field along the dotted line shown in Figs. 2(a) and 2(b) ($z=h=100$ nm, $y=p/2=100$ nm) for different values of M and M'. Note that this line overhangs the defect. It is the place where the field is the most affected by the presence of the object. It is observed that, when the observation point is just above the defect, the calculation with $M=M'=3$ is very close to that obtained with $M=M'=5$ and $M=M'=11$ (the convergence rate is quick). On the other hand, if the observation point moves away from the defect,

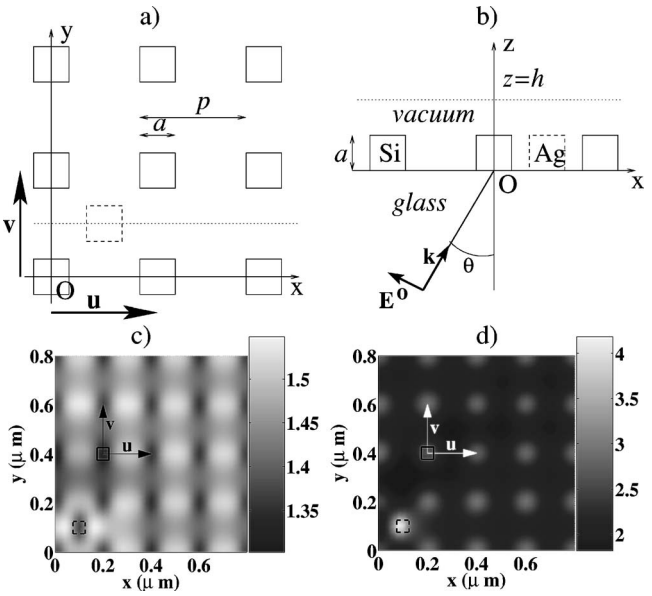

FIG. 2. (a) and (b) top view and side view of the geometry of the system: the double-periodic structure is formed by pads in silicon with size a^3, and a square periods p. The defect is a silver pad with the same size (a^3), and the wavelength of the TM polarized illumination is $\lambda=600$ nm. (c) Near field intensity for $a=50$ nm, $p=200$ nm, $h=100$ nm, and $\theta=0^\circ$. (d) Near-field intensity for $a=50$ nm, $p=200$ nm, $h=100$ nm, and $\theta=50^\circ$.

the value obtained for $M=M'=3$ departs from that given with $M=M'=5$ and $M=M'=11$. This result is in agreement with the previous discussion on the influence of the "parasite dipoles" which increases when the observation point is far from the object. Note that, as expected, in the converged cases, as the point of observation moves away from the defect, the intensity comes closer to that obtained for the grating without the defect.

If the observation point is in far field [Figs. 3(c) and 3(d)] the sensibility to the number of modes M and M' is very small due to the accurate evaluation of the far field with the reciprocity theorem. In this case, the mode numbers influences solely the calculation of the field inside the defect and the convergence of this near-field calculation is obtained with a relatively small number of modes. For comparison purpose, we also plot in the solid line the field scattered by the defect alone on the substrate. In this example, we observe that the grating does not modify the field scattered by the defect in far field. This means that the coupling between the defect (silver pad) and the silicon pads of the grating is weak. In Fig. 4 the same study is conducted for a smaller period of the grating, $p=100$ nm, so that a stronger coupling is expected. The same observations as that done for the previous Figs. 3(a) and 3(b) can be done for Figs. 4(a) and 4(b) except that the convergence is obtained for a significantly higher number of modes $M=M'=21$. This was to be expected since the period of the grating is smaller. In the far-field case, Figs. 4(c) and 4(d), we observe that the field scattered by the defect in the presence of the grating differs strongly from that scattered by the defect alone on the substrate; this implies a strong coupling between the defect and the grating. Note that, contrary to the near-field calculation, the convergence is

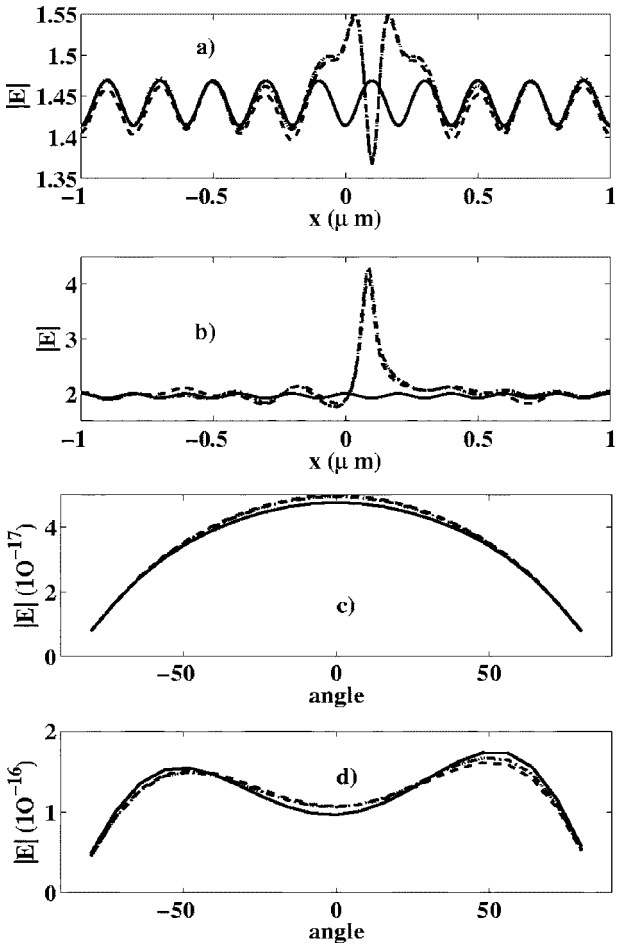

FIG. 3. We present the modulus of the field in the near-field [(a) and (b)] and in the far-field zone [(c) and (d)]. Computations done with $M=M'=3$ are in the dashed line, for $M=M'=5$ in the dot-dashed line, and for $M=M'=11$ in the dotted line. (a) and (b) modulus of the field in the near-field zone: $z=h=100$ nm, and $y=p/2=100$ nm. In plain line the field obtained without the defect (a) $\theta=0^\circ$. (b) $\theta=50^\circ$. (c) and (d) modulus of the field in the far-field zone $y=0$ and $x^2+z^2=1$ m, and in the solid line the field scattered by the defect without the double-periodic structure (c) $\theta=0^\circ$. (d) $\theta=50^\circ$.

almost reached for $M=M'=3$. The evaluation of the far-field amplitude does not necessitate an accurate calculation of the near field. Indeed, the propagation in vacuum is a low-pass filter, so that the high-frequency components of the near field (that are the most difficult to calculate accurately) are suppressed. Hence very few modes are necessary to evaluate the far-field scattered by the defect.

In Fig. 5, we study the number of duplicated motifs that are necessary to simulate the presence of an infinite grating and we compare the results to that of our method. The structure under study is the same as that of Fig. 4 and it is illuminated under normal incidence and in total internal reflection configuration $\theta=50^\circ$. We use the classic CDM[12] to simulate the field scattered by an object consisting in a silver cube surrounded by a finite number of silicon cubes, i.e., we truncate the sums in Eq. (1): $\Sigma_{m,n=-\infty}^{\infty} \approx \Sigma_{m,n=-M_{\max}}^{M_{\max}}$. Note that the linear system that has to be solved in this case is quite

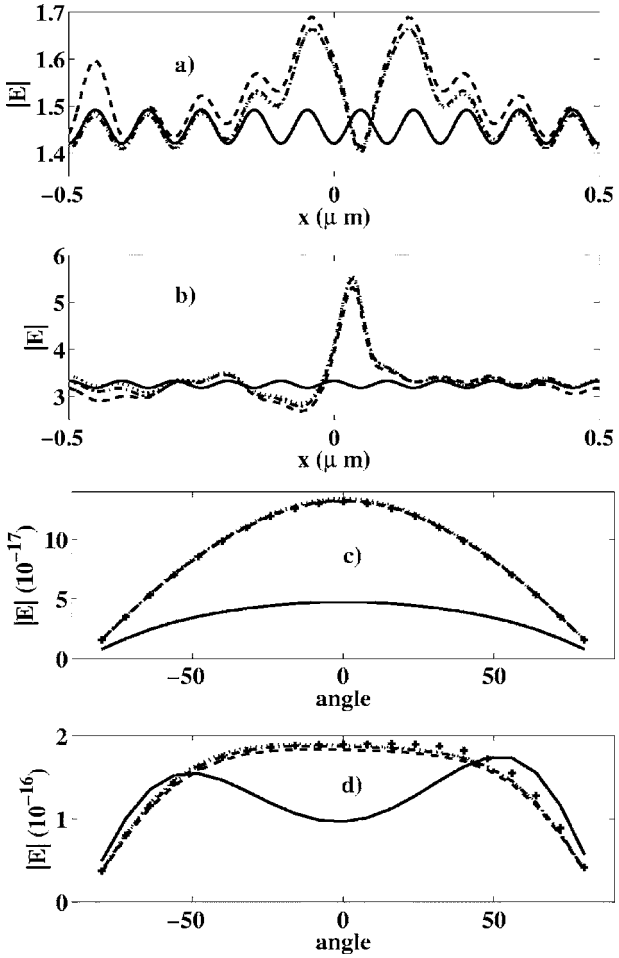

FIG. 4. We present the modulus of the field in the near-field [(a) and (b)] and in the far-field zone [(c) and (d)]. Computations done with $M=M'=3$ are indicated with crosses [not represented in (a) and (b)], for $M=M'=5$ in the dashed line, for $M=M'=11$ in the dot-dashed line, and $M=M'=21$ in the dotted line. (a) and (b) modulus of the field in near field zone: $z=h=100$ nm, and $y=p/2=50$ nm. In the solid line the field obtained without the defect. (a) $\theta=0^\circ$. (b) $\theta=50^\circ$. (c) and (d) modulus of the field in the far-field zone $y=0$ and $x^2+z^2=1$ m, and in the solid line the field scattered by the defect without the double-periodic structure (c) $\theta=0^\circ$. (d) $\theta=50^\circ$.

large (for example, 1600 base cells for $M_{\max}=20$). In Fig. 5 we compare the near field above the defect, in the presence of the infinite grating and for various truncated gratings. The number of periods, $M_{\max}$, is successively equal to 0 (object alone, dotted line), $M_{\max}=5$ (dashed line), and $M_{\max}=20$ (solid line). The field scattered by the defect in the presence of the infinite structure is represented by the bold line. For the angle of incidence $\theta=50^\circ$, Fig. 4, we observe that more than $M_{\max}=20$ is necessary to reproduce the influence of the infinite grating. Under normal incidence, the convergence is reached more easily but still, five periods are not enough to give a good estimation of the field. This numerical test permits the validation of our method and it shows the difficulty of replacing the infinite grating by a truncated one. Note that the time of computation with the classic CDM and the truncated grating with $M_{\max}=20$ is 25 times larger than that of our technique.

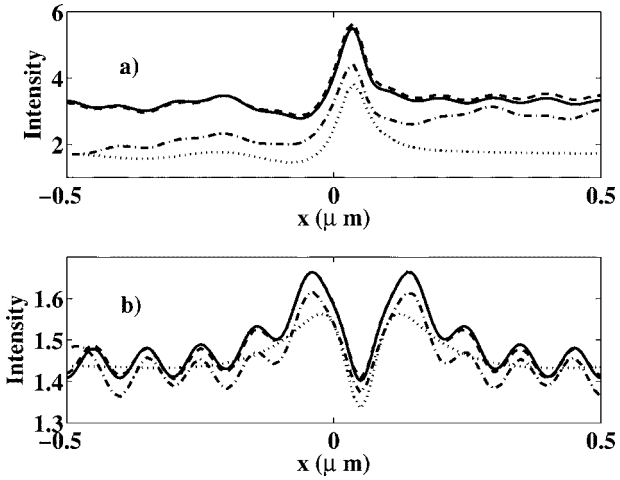

FIG. 5. The configuration used for these curves is the same as the one used in Fig. 4. In the solid line the computation is done as in Fig. 4 with $M=M'=11$. The other curves are obtained by truncating the infinite sum in Eq. (1). The curve in the dotted line is obtained for the object alone ($M_{\max}=0$), in the dot-dashed line with $M_{\max}=5$, and in the dashed line with $M_{\max}=20$ ($M_{\max}$ is defined in the text). (a) $\theta=50^\circ$. (b) $\theta=0^\circ$.

In Fig. 6 we give different examples of the wide possibilities of our method. We keep the same grating as that of Fig. 2 with $p=100$ nm and we change the nature of the defect. All the calculations are performed with $M=M'=11$ since Fig. 4 has shown that convergence had been reached in this case. In Figs. 6(a) and 6(b) we remove a silicon cube [we create a lacuna with an aperiodic object with negative polarizability, opposite to that of the grating, $\alpha_d(\bar{\mathbf{r}}_j)=-\alpha_{Si}(\bar{\mathbf{r}}_j)$]. In Figs. 6(c) and 6(d) the silicon cube at the center of the image is replaced by a silver cube $\alpha_d(\bar{\mathbf{r}}_j)=-\alpha_{Si}(\bar{\mathbf{r}}_j)+\alpha_{Ag}(\bar{\mathbf{r}}_j)$. In Figs. 6(e) and 6(f) the silicon cube at the center of the image is moved at the position $(p/2)\mathbf{u}+(p/2)\mathbf{v}$; the method consists in that case to first cancel one silicon cube by creating a lacuna then adding a cube in silicon at the new position. Note that all these different examples are easily computed once the field susceptibility tensor of the grating is known. When the illumination is normal to the substrate in Figs. 6(a), 6(c), and 6(e), the incident electric field is directed along the x axis. Assuming that the field direction in the structure is close to that of the transmitted incident field, one can explain the pattern of the near-field intensity by invoking the continuity of the field displacement $\mathbf{D}=\varepsilon\mathbf{E}$ along the x axis, (where ε is either the permittivity of vacuum or that of silicon), and the continuity of $\mathbf{E}$ along the y axis. As expected, the field minimum is found inside the silicon pads, and, by continuity, this low field is retrieved along lines oriented along the y axis. The minimum of intensity above the silicon pads neighboring the lacuna on the left and right can also be explained by invoking the continuity of the field displacement. In Fig. 6(c), the central silicon pad has been replaced by a silver pad. The resulting map of intensity is close to that of the unperturbed grating. Indeed, at this wavelength the permittivity of silver is close to that of silicon in

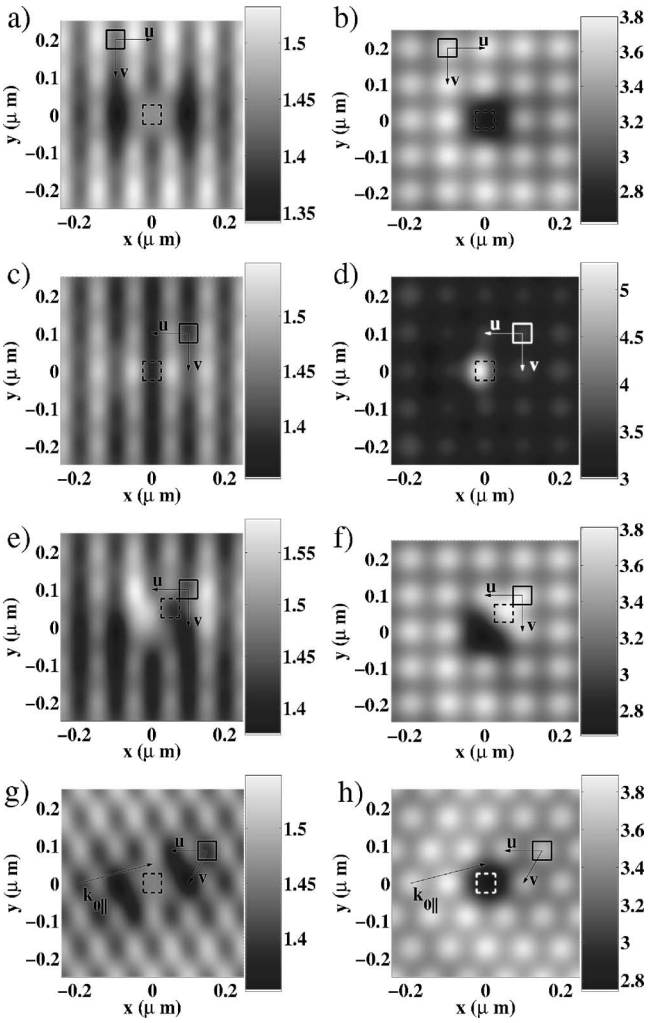

FIG. 6. Near-field images obtained from a double-periodic structure as described in Fig. 2 with $p=100$ nm, $a=50$ nm, $\mathbf{k}_{0\|}$ along the x axis for the first six images, and with $\mathbf{u}=(100,0)$ nm, $\mathbf{v}=(50,86)$ nm, $\mathbf{k}_{0\|}$ as showed in the figure for images (g) and (h). The square in the solid line represents the base cell and $\mathbf{u}$ and $\mathbf{v}$ represent the basis vector of the double-periodic structure. We have taken $h=100$ nm, and $\lambda=600$ nm, and the pads are in silicon. (a), (c), (e), and (g) are obtained for $\theta=0°$. (b), (d), (f), and (h) are obtained for $\theta=50°$. (a), (b), (g), and (h) the square in dashed line represents a lacuna in the double-periodic structure. (c) and (d) the square in the dashed line is in silver. (e) and (f) the square in dashed line is a pad of silicon that has been displaced in the double-periodic structure.

absolute value ($\varepsilon_{Ag}=-13+0.9i$ instead of $\varepsilon_{Si}=15+0.2i$). Hence one expects the intensity inside the silver pad to be similar to that existing in a silicon pad. As a consequence, the intensity map is not strongly modified by the presence of this defect in the grating. In Figs. 6(b), 6(d), and 6(f), the incident angle is $\theta=50°$, hence the transmitted incident field is mostly directed along the z axis and it decays exponentially quicker in air than in silicon. This might explain why the field above the lacuna is smaller than the field above the silicon pads in all these plots. The enhancement of the field above the silver pad can be due to the fact that the polarizability of the silver pad is bigger than that of the silicon pad, so that the radiated field by the defect is stronger than that radiated by a base cell of the grating. In Figs. 6(g) and 6(h), we have changed the grating and taken a triangular lattice [$\mathbf{u}=(100,0)$ nm and $\mathbf{v}=(50,86)$ nm]. The defect consists in a lacuna at the origin. The illumination is chosen so that there is an angle of 10° between the x axis and $\mathbf{k}_{0\|}$. To explain the main features of the intensity map, the same comment as that given for Figs. 6(a) and 6(b) holds also in this case.

IV. CONCLUSION

We have proposed a rigorous numerical technique based on the principles of the coupled dipole method, that permits the simulation of the field scattered by an object embedded in a planar periodic structure. We have presented an efficient means to calculate the field radiated by a dipole in the presence of a grating both in near and far field and studied carefully the convergence of the technique. The advantage of our method is that it addresses any kind of inhomogeneous objects and gratings (in particular the object can be a lacuna). Moreover, in this paper, the periodic structure was deposited on flat homogeneous substrate, but the latter could easily be replaced by a multilayer (that supports guided waves, for example). Once the field susceptibility tensor of the grating is known, the computation cost of the method depends solely on the size of the object compared to the wavelength. It is thus possible to study rapidly many kinds of defects. This method should be very useful for designing optical planar components using cavities in slices of two-dimensional photonic crystal.[20,21]

APPENDIX A: FIELD DIFFRACTED BY THE GRATING IN ABSENCE OF THE DEFECT

Once the field susceptibility tensor of the double-periodic structure is known for any pair of points $(\mathbf{r},\mathbf{r}')$, the field can be evaluated at any position $\mathbf{r}$ by solving the linear system Eq. (4) and using Eq. (5). The last step is then to evaluate the field that would exist in the absence of the defect, $\mathbf{E}_{per}$. The incident beam being a plane wave, $\mathbf{E}_{per}$ can be obtained by any grating methods.[3] With our formulation $\mathbf{E}_{per}$ is simply given through

$$\mathbf{E}_{per}(\bar{\mathbf{r}}_j)=\mathbf{E}^0(\bar{\mathbf{r}}_j)+\sum_{l=1}^{N}\mathbf{S}_{per}(\bar{\mathbf{r}}_j,\bar{\mathbf{r}}_l,\mathbf{k}_{0\|})\alpha_p(\bar{\mathbf{r}}_l)\mathbf{E}_{per}(\bar{\mathbf{r}}_l), \tag{A1}$$

with $j=1,\ldots,N$. To obtain Eq. (A1) we have used the fact that the substrate is illuminated by a plane wave whose wave vector $\mathbf{k}_0$, projected onto the $(\mathbf{u},\mathbf{v})$ plane is $\mathbf{k}_{0\|}$ so that

$$\mathbf{E}^0(\bar{\mathbf{r}}_i+m\mathbf{u}+n\mathbf{v})=\mathbf{E}^0(\bar{\mathbf{r}}_i)\exp[i\mathbf{k}_{0\|}.(m\mathbf{u}+n\mathbf{v})]. \tag{A2}$$

The linear system (of size $3N\times 3N$) represented by Eq. (A1) is easy to solve, and then the electric field due to the double-periodic structure can be computed at any arbitrary position $\mathbf{r}$:

$$\mathbf{E}_{\mathrm{per}}(\mathbf{r}) = \mathbf{E}^0(\mathbf{r}) + \sum_{j=1}^{N} \mathbf{S}_{\mathrm{per}}(\mathbf{r}, \bar{\mathbf{r}}_j, \mathbf{k}_{0\|}) \alpha_{\mathrm{p}}(\bar{\mathbf{r}}_j) \mathbf{E}_{\mathrm{per}}(\bar{\mathbf{r}}_j). \quad \text{(A3)}$$

More details on the numerical evaluation of $\mathbf{E}_{\mathrm{per}}$ can be found in Ref. 3.

APPENDIX B: EFFICIENT COMPUTATION OF THE MAP OF $\mathbf{E}_{\mathrm{per}}(\mathbf{r})$

In this appendix we propose an efficient way to compute $\mathbf{E}_{\mathrm{per}}(\mathbf{r})$ for many positions above the grating with the coupled dipole method. This technique can be useful to obtain the map of the field at different altitudes (for near-field microscopy experiments, for example). Using the previous appendix, we calculate the field on the surface of the base cell at a constant altitude z above the grating. Bearing in mind the pseudoperiodicity of the field, we cast the latter into a Fourier series,

$$\mathbf{E}_{\mathrm{per}}(\mathbf{r}_\|, z) = e^{i\mathbf{k}_{0\|}\cdot\mathbf{r}_\|} \sum_{m,n=-\infty}^{\infty} \boldsymbol{\mathcal{E}}_{m,n}(\mathbf{k}_{0\|}, z) e^{i(m\mathbf{U}+n\mathbf{V})\cdot\mathbf{r}_\|}, \quad \text{(B1)}$$

with

$$\boldsymbol{\mathcal{E}}_{m,n}(\mathbf{k}_{0\|}, z) = \frac{1}{|\mathbf{u}\times\mathbf{v}|} \int\int_{\mathrm{Cell}} \mathbf{E}_{\mathrm{per}}(\mathbf{r}_\|, z) e^{-i(\mathbf{k}_{0\|}+m\mathbf{U}+n\mathbf{V})\cdot\mathbf{r}_\|} d\mathbf{r}_\|. \quad \text{(B2)}$$

Once the modes $\boldsymbol{\mathcal{E}}_{m,n}(\mathbf{k}_{0\|}, z)$ are known, one obtains the field above the double-periodic structure at any altitude z' above the grating with

$$\mathbf{E}_{\mathrm{per}}(\mathbf{r}_\|, z') = e^{i\mathbf{k}_{0\|}\cdot\mathbf{r}_\|} \sum_{m,n=-\infty}^{\infty} \boldsymbol{\mathcal{E}}_{m,n}(\mathbf{k}_{0\|}, z) e^{[i(m\mathbf{U}+n\mathbf{V})\cdot\mathbf{r}_\| + \gamma_{m,n}(z'-z)]}, \quad \text{(B3)}$$

with $\gamma_{m,n} = [k_0^2 - |\mathbf{k}_{0\|} + m\mathbf{U} + n\mathbf{V}|^2]^{1/2}$.

[1] H. Rigneault, F. Lemarchand, and A. Sentenac, J. Opt. Soc. Am. A **17**, 1048 (2000).
[2] F. M. Kahnert, J. Quant. Spectrosc. Radiat. Transf. **79-80**, 775 (2003).
[3] P. C. Chaumet, A. Rahmani, and G. W. Bryant, Phys. Rev. B **67**, 165404 (2003).
[4] E. Popov, M. Nevière, B. Gralak, and G. Tayeb, J. Opt. Soc. Am. A **19**, 33 (2002), and references therein.
[5] C. T. Chan, Q. L. Yu, and K. M. Ho, Phys. Rev. B **51**, 16635 (1995).
[6] R. D. Meade, A. M. Rappe, K. D. Brommer, J. D. Joannopoulos, and O. L. Alherhand, Phys. Rev. B **48**, 8434 (1993); **55**, 15942 (1993).
[7] M. Okano, A. Chutinan, and S. Noda, Phys. Rev. B **66**, 165211 (2002).
[8] P. C. Chaumet, A. Sentenac, and A. Rahmani, Phys. Rev. E **70**, 036606 (2004).
[9] E. M. Purcell and C. R. Pennypacker, Astrophys. J. **186**, 705 (1973).
[10] B. T. Draine, Astrophys. J. **333**, 848 (1988); B. T. Draine and J. Goodman, *ibid.* **405**, 685 (1993), and references therein.
[11] R. Schmehl, B. M. Nebeker, and E. D. Hirleman, J. Opt. Soc. Am. A **14**, 3026 (1997).
[12] P. C. Chaumet and M. Nieto-Vesperinas, Phys. Rev. B **61**, 14119 (2000); **62**, 11185 (2000); **64**, 035422 (2001).
[13] A. Rahmani, P. C. Chaumet, and F. de Fornel, Phys. Rev. A **63**, 023819 (2001).
[14] J. D. Jackson, *Classical Electrodynamics*, 2nd ed. (John Wiley, New York, 1975), p. 395.
[15] P. C. Chaumet and M. Nieto-Vesperinas, Opt. Lett. **25**, 1065 (2000).
[16] P. C. Chaumet, Appl. Opt. **43**, 1825 (2004).
[17] G. P. M. Poppe, C. M. J. Wijers, and A. van Silfhout, Phys. Rev. B **44**, 7917 (1991).
[18] S. Seely and A. D. Poularikas, *Electromagnetics Classical and Modern Theory and Applications*, (Marcel Dekker, New York, 1979).
[19] *Handbook of Optical Constants of Solids*, edited by E. D. Palik (Academic Press, New York, 1985).
[20] C. Sauvan, P. Lalanne, and J. P. Hugonin, Phys. Rev. B **71**, 165118 (2005).
[21] N. Louvion, D. Gérard, J. Mouette, F. de Fornel, C. Seassal, X. Letartre, A. Rahmani, and S. Callard, Phys. Rev. Lett. **94**, 113907 (2005).